AN OPTIMAL HEATING METHOD USING TE-WAVE-RADIATING HYPERTHERMIA APPLICATORS BASED ON THE FD-TD ANALYSIS

Nagayoshi MORITA, Takuji IKEDA, and Koji MORIMOTO
Department of Communication Engineering, Faculty of Engineering
Osaka University, Suita, Osaka 565, Japan

INTRODUCTION

In hyperthermia treatment, efficient, noninvasive, and focalized heating is most desirable and ideal. For heating superficial tumors, these conditions can comparatively easily be attained, e.g., by using microwave applicators. For heating deep-seated tumors, however, it is very difficult to achieve such ideal heating conditions because of the electrical properties of the human body. Applicators of the capacitive type and the inductive type, and the Annular Phased Array System (APAS) would be typical three types of applicators developed for the purpose of heating noninvasively deep inside the body. Although these applicators have been used for clinical trials in many hospitals, each of them has its respective drawbacks, particularly in the viewpoint of selective heating. Endeavors not only to improve these applicators operationally and technologically but also to develop new types of applicators have been continued.

A new type of multiapplicator system we have proposed [1] is composed of several antennas radiating a Transverse Electric (TE) wave, where the human body is assumed to be of a cylindrical shape. This applicator system has both advantages of the capacitive type applicator, possible to limit heating regions in the axial direction, and of APAS, able to make use of coherency of electromagnetic waves in the cross-sectional plane. For making the best use of this applicator system, it is desirable to control the excitation amplitude and phase of each applicator element, so as to form a hot zone around the tumor region. A very simple optimization scheme is available for this purpose [2], if we can analyze accurately the problem of TE wave scattering from inhomogeneous lossy cylinders. Several numerical methods would be utilized for this analysis to be done. We invoke here the FD-TD method [3,4], which seems to be the most pertinent one for the present usage.

Numerical results of power loss patterns and electric field vector patterns are presented for a typical model of the human abdomen heated by the TE-wave-radiating applicator system with excitation amplitudes and phases being controlled optimally.

MODEL FOR THE HUMAN ABDOMEN AND APPLICATORS

Figure 1 represents the models of the human abdomen and applicators, both uniform in the z-direction, together with the lattice used for FD-TD analysis. Regions (I) and (II) are the media with electrical constants of bone and muscle, respectively, and the outside of region (II) is assumed to be filled with water. The form of regions (I) and (II) in Fig.1 was modeled on Fig.2, a simplified sketch of a CT-image of the adrenal-kidney level of the human abdomen. The lattice interval is taken to be 1 cm in both x- and y-directions. The applicator system is composed of four element antennas radiating the TE wave. Each element is represented by a set of line sources corresponding to magnetic field H_z^i and electric fields E_x^i and E_y^i, as detailed in Fig.3. All H_z^i in each element are in phase, so also all $\mathbf{E}^i$, and the relation between H_z^i and $\mathbf{E}^i$ is subject to

that of a plane wave. The direction of radiation can be changed by adjusting relative excitation phases between E_x^i and E_y^i.

THE OPTIMIZATION SCHEME

With $h_n(\rho)$ being the z-component of the magnetic field generated by the n-th element antenna, the z-component of the total magnetic field $H(\rho)$ is given by

$$H(\rho) = \sum_{n=1}^{M} a_n h_n(\rho) \qquad (1)$$

where ρ is the coordinate vector, M is the number of element antennas, which is 4 in the case of Fig.1, and a_n is the complex excitation coefficient of the n-th antenna. Then, the amplitude and phase of a_n which minimizes the scalar quantity

$$\Omega = \| \bar{H}_0 - \bar{H} \|^2 \qquad (2)$$

are just the optimal excitation amplitude and phase of the n-th antenna, where $\bar{H}_0$ is the vector the components of which are the values at the pre-specified coordinate points of target magnetic field $H_0(\rho)$, $\bar{H}$ is the vector the components of which are the values at the same points of total magnetic field $H(\rho)$ defined above, and $\|\cdot\|$ denotes the vector norm. It would be very difficult to determine the target field $H_0(\rho)$. Theoretically, this field must be in the space the base functions $h_n(\rho)$ subtend. The following simple function would be suitable, though not ideal:

$$H_0(\rho) = J_1(k\rho) \cos\phi \qquad (3)$$

which is the axial component of the magnetic field of TE_{11} mode of the circular waveguide in the limit as the propagation constant tends to zero, where ρ and ϕ are the cylindrical coordinates and k is the wave number in region (II).

NUMERICAL CALCULATION

The calculation of magnetic field distribution $h_n(\rho)$ plays a major part of the whole numerical process. This calculation is done here by invoking the FD-TD method. The absorbing boundary condition of the second order [5] is applied at the outermost rectangular boundary of Fig.1.

Numerical results are presented for the following parameter and constant values: the frequency f is 100 MHz, the relative dielectric constant ε_r in regions (I), (II), and (III) are 7.45, 71.7, and 78.1, respectively, conductivity σ in regions (I), (II), and (III) are 4.36×10^{-2}, 0.889, and 0(S/m), respectively, and the time increment Δt is chosen as $(1/3)\times 10^{-10}$(s). The (x,y) coordinates of the central points of H_z^i for the four element antennas are (43.5, 31.5), (4.5, 31.5), (4.5, 7.5), and (43.5, 7.5) (all in cm).

Fig.4 shows the power loss distributions obtained by using the optimization scheme for the central point of the target distribution at (21.5, 19.5) (cm) where $\theta=\pi/4$. The positions of the specified points used for the optimization process are listed in Table 1. It is observed that the power loss becomes large considerably on the back side of the abdominal cross section. It would be necessary to cool down this portion, for instance, by water. The swelling arising in the central part near the spinal cord looks unavoidable for the case of TE wave irradiation, this being almost the same situation as for the case of capacitive type heating. Fig.5 represents the electric field vector patterns where the length of arrows is proportional to the magnitude of the electric field; (a) is the pattern at the time of just the 20th period of oscillation, and (b), (c), and (d) are those at the time when time has passed by $\pi/6$, $\pi/3$,

$\pi/2$, respectively, in terms of phase values. Careful inspection will reveal that the electromagnetic field advances inwardly as its electric vector directions whirl, and that, near bone, the electric lines of force are formed in such a manner as keeping away from the bone area. Incidentally, it was found, though not presented here, that the numerical results obtained above do not much differ from those calculated using just one line source H_z^i per each element antenna [6] instead of the set of line sources shown in Fig.3. This is because in the present problem the wavelength is very long compared with the length of source regions extending.

REFERENCES

[1]T.Ikeda, N.Morita, and N.Kumagai, Proc. 4th Annual Meeting, Jpn. Soc. Hyperthermic Oncol., 37, 1987.

[2]N.Morita, T.Hamasaki, and N.Kumagai, IEEE Trans. Microwave Theory Tech., MTT-34, pp.532-538, 1986.

[3]K.S.Yee, IEEE Trans. Antennas Propag., AP-14, pp.302-307, 1966.

[4]D.T.Borup, D.M.Sullivan, and O.P.Gandhi, IEEE Trans. Microwave Theory Tech., MTT-35, pp.383-395, 1987.

[5]G.Mur, IEEE Trans. Electromag. Compat., EMC-23, pp.377-382, 1981.

[6]K.Morimoto, T.Ikeda, and N.Morita, 1989 I.E.I.C.E. Springtime National Convention, B-4-8, 1989.

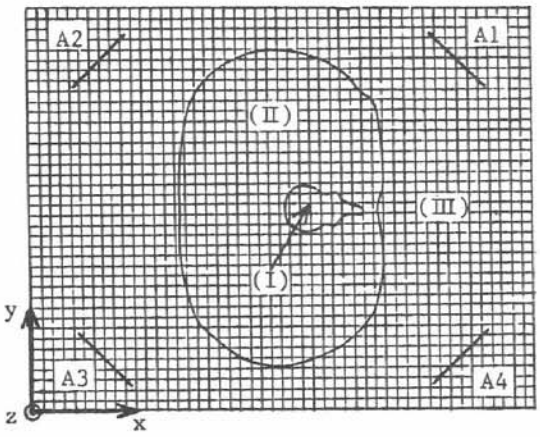

Fig.1. Models for the human abdomen and applicators together with the lattice for FD-TD analysis.

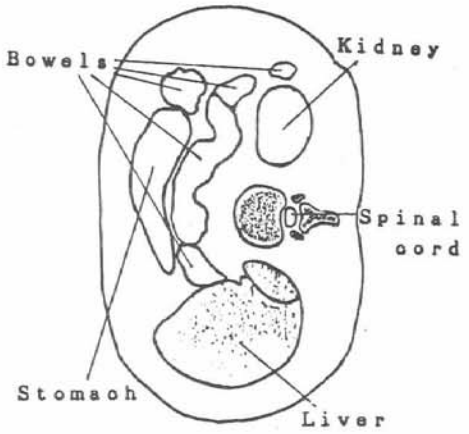

Fig.2. A sketch of a CT-image of the adrenal-kidney level.

Table 1 Coordinates of pre-specified points (in cm).

(x , y)	
(17.5, 14.5)	(17.5, 19.5)
(17.5, 24.5)	(21.5, 14.5)
(21.5, 19.5)	(21.5, 24.5)
(25.5, 14.5)	(25.5, 24.5)

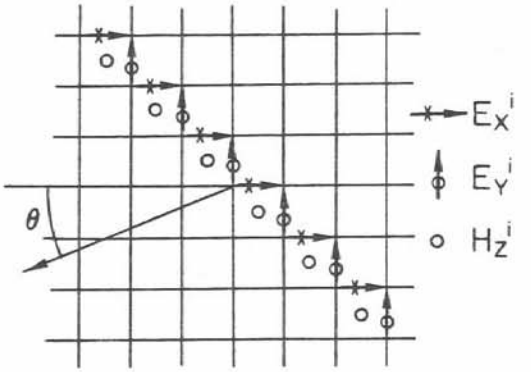

Fig.3. A set of line sources for modeling applicators.

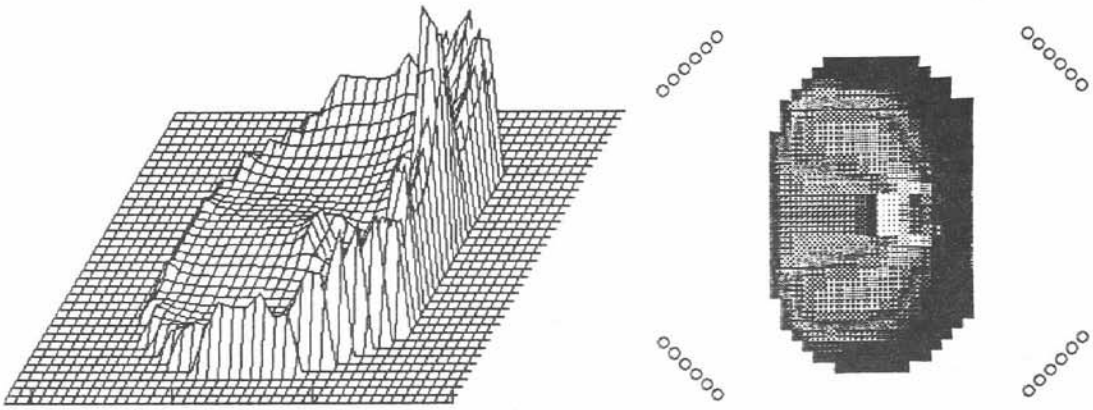

(a) A three-dimensional sketch

(b) A chialoscuro sketch

Fig.4. Power loss distributions.

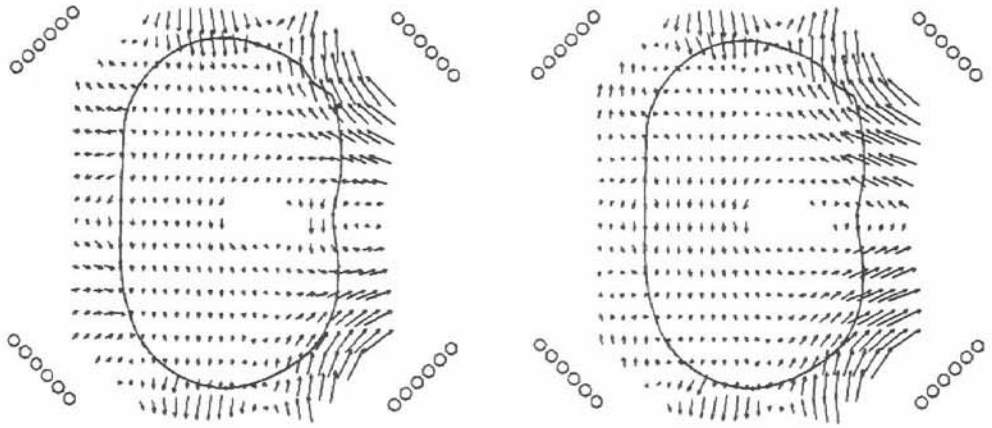

(a) At 20th period

(b) π/6 afterwards

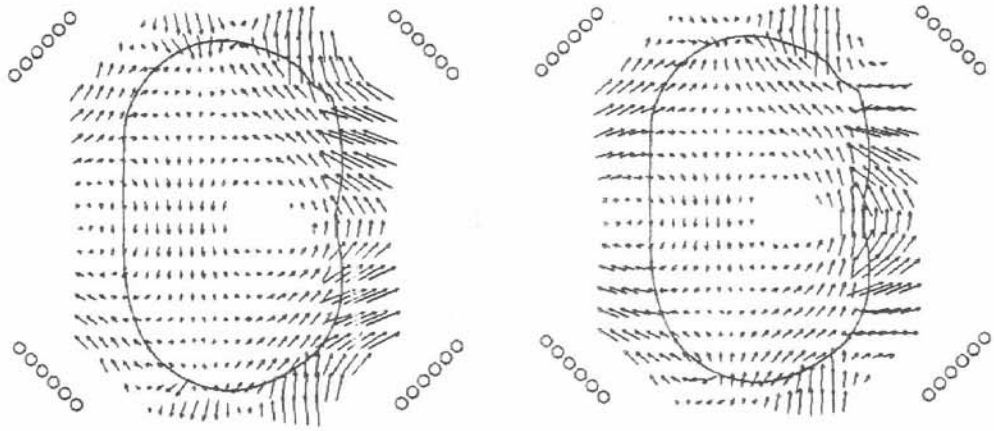

(c) π/3 afterwards

(d) π/2 afterwards

Fig.5. Electric field vector patterns.